

Venus Surface AM Radio Link Analysis: Preliminary Study

David D. Morabito,* Mohammad Ashtijou,† Thaddaeus Voss,‡ and Joseph Vacchione‡

ABSTRACT. — This study examines link analyses involving a lander on the surface of Venus where high atmospheric temperature and pressure are not conducive to the use of modern-day digital electronics. We explore the use of older analog technology such as AM/FM radio, which is more amenable to Venusian surface conditions. The lander will have a communications link to an orbiting spacecraft at an altitude of 240 km, which will receive the lander's transmitted signal. The orbiter will perform the necessary conditioning and processing of the received signal and package it for relay back to Earth on an interplanetary link. The visibility time per a particular orbit is on the order of a few minutes. We consider three scenarios for returning the data to Earth: 1) On-board processing and detection of signal frequencies on the orbiter to be telemetered back to Earth; 2) Reception of the full 1-MHz analog band at the orbiter which in turn gets sampled, digitized, and encoded for transmission back to Earth; and 3) Reception of the full 1-MHz band directly back to Earth to be recorded on an open-loop receiver and processed in non-real time.

For scenario 1: If one makes use of 100 sensors whose frequencies are detected using onboard processing at the orbiter receiver within the 1-MHz bandwidth, then one would have a data rate of 1400 bps, assuming 14 bit/sample resolution at 1-sec updates. Note this can be further refined as the design evolves. Thus, for N sensors, we would have a $14 \times N$ bps data rate.

For scenario 2: If one wishes to ship the entire 1-MHz band received at the orbiter back to Earth, this would involve down-conversion, digital sampling at the Nyquist rate (for 2 bit/sample), and encoding with a rate $\frac{1}{2}$ error-correcting code resulting in an effective ~ 4 Msps rate back to Earth for later processing and detection of the sensor data. This is a very high data rate and the feasibility of achieving it needs to be assessed on the Venus-Earth relay link, as well as evaluating on-board storage of the recorded data between orbits.

For scenario 3: A direct-to-Earth (DTE) link from the lander to a DSN 70-m station is feasible at L-band at a frequency of 1.67 GHz, as there exists available equipment.

* Communications Architectures and Research Section.

† Radar Science and Engineering Section.

‡ Flight Communications Systems Section.

Reasonable power levels are achieved for this option for the case of six sensors (six AM sidetones), which will be discussed here.

I. Introduction

This study discusses the link analysis involving the deployment of a lander to the surface of Venus where the high atmospheric temperature and pressure are not conducive to making optimal inexpensive use of modern-day digital electronics. The atmosphere on the surface of Venus has a pressure of almost 100 times that of Earth, while the surface temperature is $\sim 900^{\circ}\text{F}$ ($\sim 460^{\circ}\text{C}$) with very little difference between day and night and with season, as compared to Earth surface temperatures that lie well below the maximum 134.1°F (56.7°C) reported so far recorded on the Earth's surface [1]. Modern-day solid-state electronic components (silicon-based semiconductors) are unable to withstand hostile Venusian surface conditions without appropriate climatic conditioning systems whose costs could range anywhere from very high to prohibitive. A study conducted at the NASA Glenn Research Center (GRC) involved a high-temperature electronics design that was based on silicon carbide (SiC) semiconductors. This study demonstrated that such SiC-based circuits could operate at Venusian surface temperatures for up to several thousand hours [2]. Early imaging from the surface of Venus was performed by the Russian Venera landers in the 1960s and 1970s. According to the available literature [3–5], Venera-9 imaged the surface of Venus using an FM system at 256 bits/sec on two separate camera channels, possibly using vacuum tube “digital” circuits.

There are numerous instances in the literature on the performance of non-digital telemetry from the 1930s onward, such as multitone systems where telemetry involved the use of multiple FM or AM subcarriers. The Inter-Range Instrumentation Group (IRIG) provides recommendations in the form of standards for analog FM systems such as those that deal with frequency division multiplexing and subcarriers, although they emphasize that digital systems have now largely superseded the use of analog systems [6]. Other references that discuss such practices can be found in Uglow [7–8]. Previous work conducted at JPL includes a report on the use of FM telemetry involving the early Explorer missions [9]. Other early JPL work involved balloon flights and dropsondes of various kinds that many times made use of FM analog telemetry [10]. The old Microlock system essentially received FM telemetry from very simple electronics in the spacecraft. This previously made use of FM on subcarriers, modulated onto a carrier, somewhat similar to modern day DSN telemetry, which, however, makes use of phase modulation. The experiment made use of a 10-kW power amplifier, with a 310K Exciter Modulator on the ground for transmission, and, for receiving, an ARPA 108 MHz Microlock Receiver that was converted to 955 MHz [11].

In this study, we explore the use of older analog systems such as vacuum tube technology used for AM/FM radio communications, where its application is amenable to the Venusian surface conditions. Here, we assume a totally analog transmitter system involving frequency-calibrated sensors feeding an AM modulator (double-sideband). For the transmitter, one could possibly make use of a vacuum tube oscillator (which would not require any heater power). The resonant frequency could be controlled by a temperature-dependent component such as a resonant cavity. One could also make use of Silicon-

Carbide (SiC) semiconductors which have been demonstrated to operate in such extreme conditions [2].

Other options have been identified for later study such as single-sideband AM and analog FM. We consider this case for lander design as a possible very-low-cost system that could team with a multi-purpose orbiter for its relay link. Much of what follows involves the link analysis assuming a DSB-AM system.

The lander will have a communications link to an orbiting spacecraft at a 240-km altitude which will receive the lander's transmitted signal. The orbiter will perform the necessary conditioning and processing of the received signal and package it for relay back to Earth on an interplanetary link. The visibility during a particular orbit for the 240-km altitude would only be a few minutes, so the strategy of sending up the signal from the lander would need to be carefully designed, also taking the expected lifetime of the lander system into account. However, a DTE link could be maintained over several hours or several days by alternating tracks between DSN stations.

For the case of atmospheric losses and hotbody noise, we make use of the formulation provided in [12]. The signal uplinked by the lander will experience attenuation due to the Venusian atmosphere, which we conservatively cap off at 5 dB at a 10-deg elevation angle and a 1-GHz frequency based on formulation provided in [12]. We also account for hotbody noise by adding an additional 600 K to the receiver noise temperature at the orbiter receiver based on the brightness temperature provided in Table 3 in [12]. The actual hotbody noise level may be lower depending upon the integration of the orbiter antenna beam (footprint) on the Venusian surface. Scenarios involving the DTE link to a DSN station will involve differing amounts of hotbody noise depending on Venus-Earth distance, DSN antenna size and link frequency. In addition, we also make use of more conservative link margins given the higher uncertainty of the link.

II. Hardware and Signal Design Assumptions

A. Lander and Orbiter Radio System Designs

We make many assumptions in this study. The orbiter has a 240-km altitude and a circular orbit, resulting in a few-minute visibility with the lander per orbit. The link is designed for a minimum 20-deg elevation angle with 622-km range distance and 1-GHz frequency. The intervening link will have an atmospheric attenuation of 5 dB at 20-deg elevation at a frequency of 1 GHz (this is very conservative and can perhaps be lowered, see [12]). We thus retain a worst-case 5-dB attenuation evaluated at 10 deg for the 20-deg links at this time. Due to large uncertainties, we also carry a 10-dB margin on the surface-to-orbiter link. For the case of a direct-to-Earth (DTE) communication link, one could consider placing the lander at an optimum location on the Venusian surface such that the local elevation angle remains very high, allowing the Venus atmospheric attenuation assumption to be set to 1 dB or lower for the frequencies being considered [12].

The lander transmitter will have RF transmit powers (P_T) of 1, 2.5, 5, and 10 W for the orbiter link (used in the trade study discussed later), and will make use of a low gain antenna (LGA) with a semi-hemispherical pattern. As a first cut example, consider a

simple, 14 cm diameter circularly polarized circular patch with a 1 cm thick “air” dielectric with an estimated mass of about 0.7 Kg. The patch style antenna is being considered first due to its low profile and its potential for robust construction. The radiation pattern is shown in Figure 1. This is a first-order estimate. Some other options and design work will be looked at in order to broaden the radiation pattern.

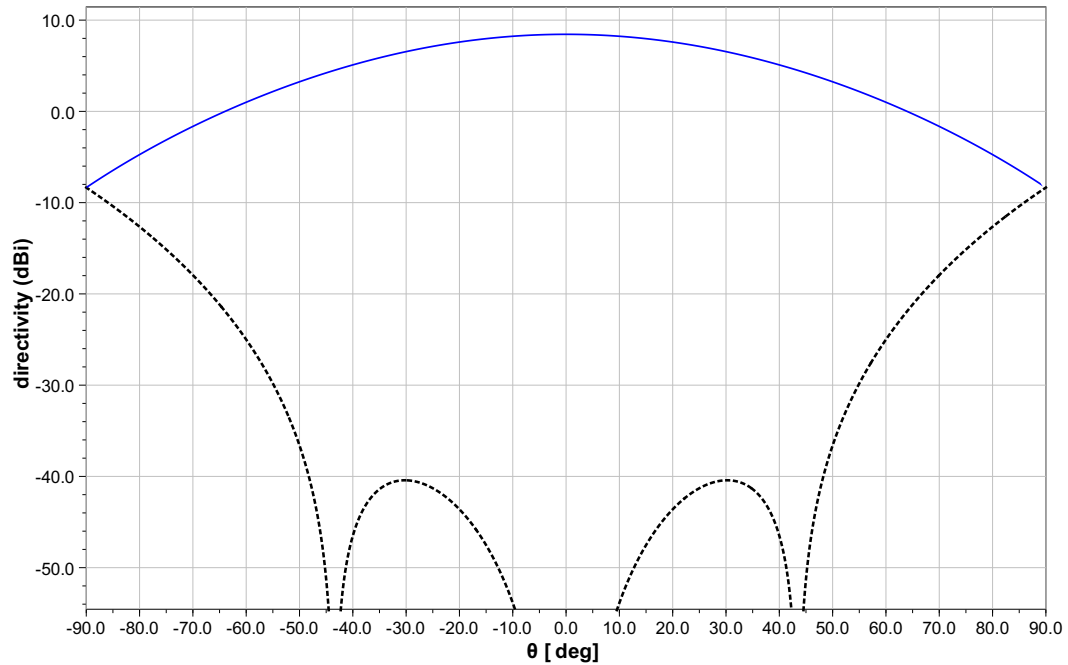


Figure 1. Lander antenna pattern for a 14.1 cm diameter circular patch with a 1 cm thick "air" dielectric at 1 GHz. Solid blue curve: Directivity for Left Hand Circular polarization (Co-pol); Dashed black curve: Directivity for Right Hand Circular polarization (Cross-pol).

Other such antenna designs currently under consideration would include a half-wave dipole (which has issues with null and positioning relative to overhead orbits), and a quarter-wave stub or monopole which has similar issues.

The system noise contributions for receiver equipment (on the orbiter) will be 277 K with an additional ~600-K maximum due to Venus hotbody noise. Actual hotbody noise encountered could be lower and would depend on the orbiter antenna footprint on the Venusian surface.

We assume a double-sideband AM system where the carrier is “stationary” in frequency and the sideband tones will have frequencies that vary with some pre-calibrated sensor quantity. We assume each sensor has its own sub-frequency band span (a few kHz each) within the overall 1-MHz band (± 0.5 MHz). There would also be accommodation for guard bands between sensor channels.

The receiver system aboard the orbiter will have an antenna with ~11-dB on-axis gain and it is assumed (for now) that it can point to the lander. At 1 GHz, such an antenna would have an effective diameter of 0.5 m if a dish design was being considered. We would likely make use of a patch array rather than the dish design (which requires a diameter spanning

a sufficient number of wavelengths). Thus, a practical design of the receive antenna would be a 2×2 patch array with a foot print of 35.8 cm by 31.0 cm and a depth of 7.1 cm. A rough estimate of mass is about 3 kg. A quadrifilar helix design would involve a length of 23 cm and a diameter of 10 cm for an on-axis gain ~ 11 dB. Designs such as a dipole or monopole have various disadvantages such as with pattern nulls, and would require judicious placement on the lander to optimize gain to preplanned relay orbits.

B. AM Radio Signal Characteristics

We assume that the transmitted carrier is always present with a constant amplitude and with an effective modulation index of m_{eff} . Once the carrier is detected and locked aboard the orbiter, a tracking bandwidth of 10 Hz is assumed sufficient (for now) to accommodate any phase noise due to the oscillator and atmospherics. Our transmitter phase noise assumption still needs to be quantified and is a focus of future work.

Figure 2 shows the block diagram of the surface transmitter that we are assuming for our system design.

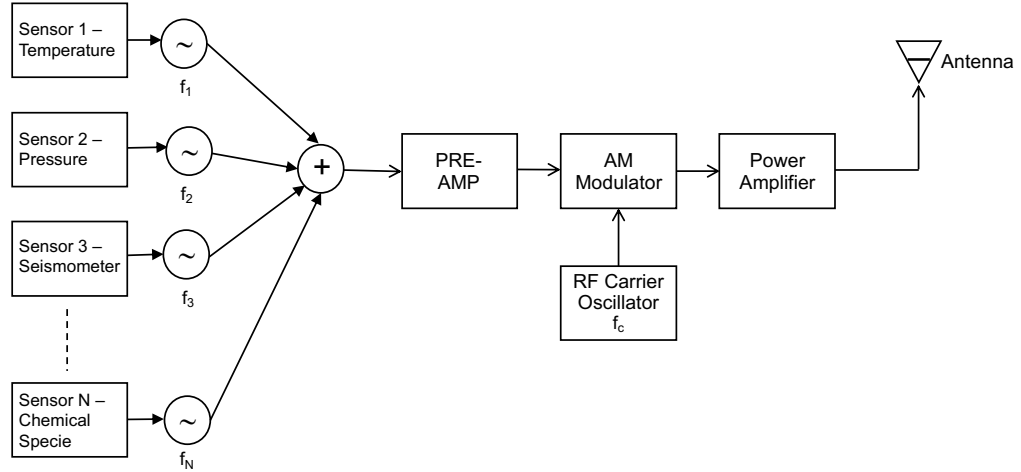


Figure 2. Block diagram for AM radio transmitter on the lander

On board the lander, we thus make use of an AM radio system, which has a total transmitted available power of P_T . Given n sensors whose signals are feeding the modulator, the effective modulation index is given by

$$m_{eff} = \sqrt{m_1^2 + m_2^2 + \dots + m_n^2} . \quad (1)$$

The power in the carrier is thus given by:

$$P_c = \frac{P_T}{1 + \frac{m_{eff}^2}{2}} . \quad (2)$$

The remaining power will be evenly split between the N sidebands where the modulation index for each sideband is m_i , and thus the power in sideband i is given by

$$P_{si} = P_c \frac{m_i^2}{2} . \quad (3)$$

It is cautioned that the higher frequency sidebands residing at the outskirts of the 1-MHz band will likely be degraded by some additional loss due to the bandpass response. Thus, one could implement a wider front-end bandwidth (e.g., 2 MHz) and just make use of the inner 1 MHz. One must also be cognizant of implementing a filter for regulatory purposes. Issues such as quantifying intermodulation distortion would also need to be considered in any such design.

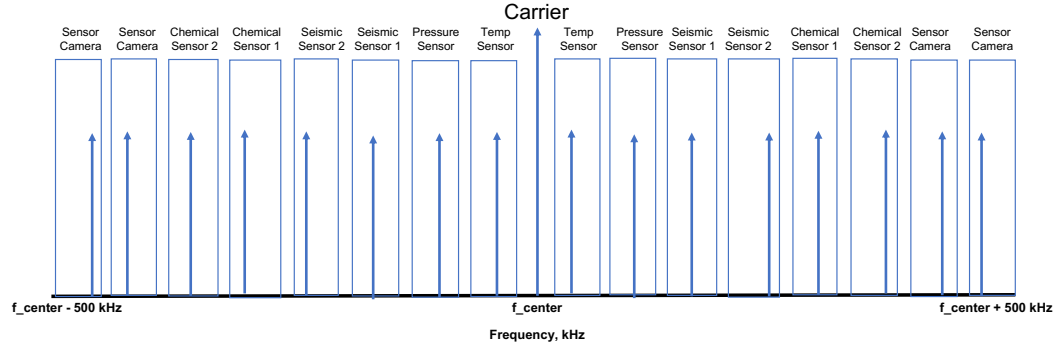


Figure 3. Example layout of carrier and sideband channels within 1 MHz bandpass assuming double-sideband AM signal.

Figure 3 displays the spectrum layout for the case of eight sensors given a double-sideband AM signal configuration. Each of the sensor readings can be represented by a frequency versus sensor quantity relationship, where the signal feeding the modulator from a particular sensor maintains a constant amplitude. The frequency-versus-sensor reading relation is pre-calibrated such that the frequency range is within the expected range of the quantity being measured. For instance, if we know that the temperature on the surface of Venus may range between 820 to 900°F, then a sensor calibrated from 750 to 950°F may suffice over the expected frequency range. If a 5 kHz band is allocated for a particular sensor, we can assume the center of this sub-band is calibrated for a temperature of 850 K, and the -2500 Hz and $+2500$ Hz outskirts are calibrated for temperatures of 750 and 950 K, respectively. Such a calibration may be performed inside a chamber simulating Venusian atmospheric conditions such as the one located at the NASA Glenn Research Center (GRC) [4, 13]. Communication system circuitry for a Venus lander designed for its hostile surface environment was developed by investigators at NASA GRC [14].

Similar schemes could be used of for other quantities such as atmospheric pressure, chemical species, and seismic sensors as well as raster scans of photographic fields-of-view (FOVs). By varying the frequency instead of amplitude, one makes use of more robust conditions. Thus, if the amplitude was varied instead, one might run into issues at the lower amplitude levels that may be more susceptible to effects such as noise or scintillation, such as could be encountered at lower elevation angles.

At the orbiter receiver, another approach involves digitally sampling the entire received 1-MHz bandwidth and packaging the data for transmission back to Earth.

We now provide some examples of AM signals using this approach. Figure 4 displays the case of standard AM where the envelope of the transmitted carrier resembles the composite of the three intelligence (or sensor) signals (10, 15, and 20 kHz). Here we have assumed an effective AM modulation index of 0.95 and carrier frequency of 2 MHz, where each intelligence signal has a modulation index of 0.55.

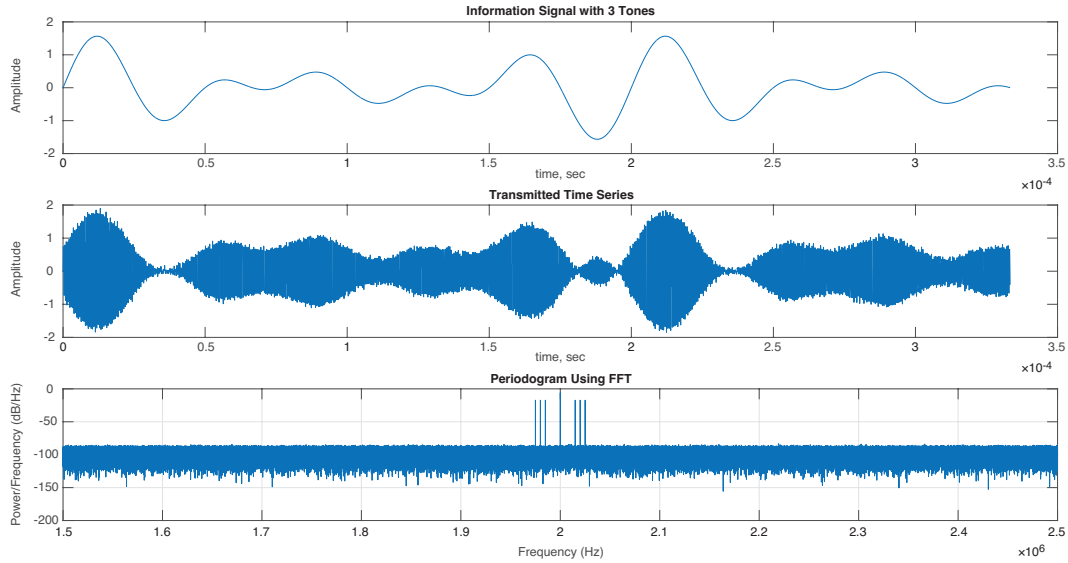


Figure 4. Top – Composite information (sideband) signal modulating the carrier for three sensor channels; Middle – Overall modulated (transmitted) AM signal relative to a center carrier frequency of 2 MHz over the 1 MHz band; Bottom – Spectra of carrier (center) and three sideband tones (on both sides of the carrier).

In Figure 5, we provide the example of an AM signal where the envelope of the transmitted carrier resembles the composite of the ten intelligence signals at 10, 15, 20, ... , 55 kHz. An effective AM modulation index of 0.95 and carrier frequency of 2 MHz is again assumed.

The appearance of intermodulation products and harmonics will begin to appear and thus their amplitudes relative to actual sideband tones will need to be characterized. Thus, a detailed study of the use of N sideband tones, their individual bandwidths, and judicious placement would need to be conducted. Given that there are short periods (very small fraction of a second) of overmodulation (and negative overmodulation), one would need to evaluate the ability of a PLL to maintain lock on the AM carrier. Thus, future work involves running the AM signal waveform through a PLL simulation to inspect what happens during those very short periods of over/under modulation.

In both cases of Figures 4 and 5, a reasonable amount of phase noise was added to raise the noise floor to more acceptable levels. The actual amount of phase noise will depend upon details of a later advanced design as these plots are provided for illustrative purposes. In addition, it is understood that the carrier frequency of 2 MHz would be the result of any downconversion from a much higher transmitted frequency on the lander-orbiter link.

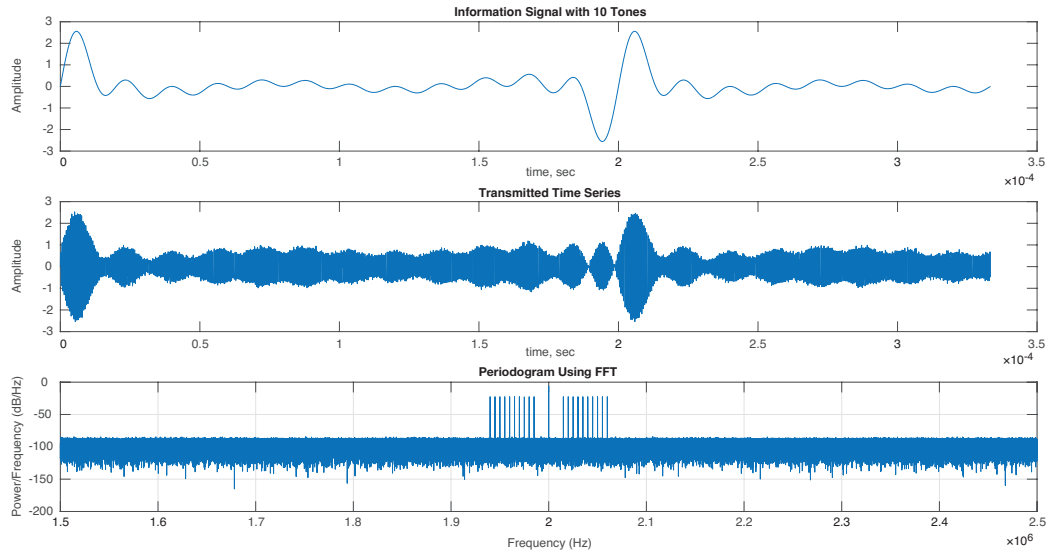


Figure 5. Top – Composite information (sideband) signal modulating the carrier based on 10 sideband channels; Middle – Overall modulated (transmitted) AM signal relative to a center carrier frequency of 2 MHz over a 1 MHz band; Bottom – Spectra of carrier (center) and ten sideband tones (on both sides of the carrier).

Given that the main signal processing scheme involves inspecting smaller bands for signal energy such as with FFT open-loop analysis, one would expect that the change in frequency for any sensor quantity would be very small over the duration of any such integration period, so that brief periods of over/under modulation would be “transparent” in the scheme. The carrier could also be “dug” out in a similar manner using spectral analysis techniques (without using the PLL approach if it does turn out to be problematic).

III. Signal Processing Schemes

We consider three possible schemes for processing the received signals from the lander. One scheme involves on-board processing at the orbiter to detect the sensor readings (Section III.A). The second scheme involves packaging the full 1-MHz band at the orbiter (centered at the down-converted carrier) for transmission to Earth for later processing (Section III.B). The third scheme involves reception of the full 1-MHz analog bandwidth on a DTE link, where it would be recorded on an open-loop receiver, to allow for specialized post-processing algorithms to detect the signals and thus the sensor readings.

A. On-Board Processing and Spectral Analysis at Orbiter (Lander to Orbiter)

The first approach would involve on-board processing. Here the AM carrier would first be detected and locked up within its known acquisition bandwidth. This step would assume the receiver has knowledge of where the carrier is located in frequency space within a sufficient guard band away from the first sensor sideband frequencies, making use of on-board frequency predicts. One could also make use of a sliding image detection approach using FFTs, enabling one to look for the comb with the right frequencies in the right places to identify the carrier tone. Once the carrier is locked, the receiver will search for each of

the N frequency sideband tones (each with their own guard bands to adjacent sensor tones) and lock onto them using appropriate signal processing techniques. Such schemes would involve performing an FFT over the 1-MHz band to detect the frequency components with largest amplitudes or use a series of several tracking loops to locate peak signals within each sensor band. Thus, the outputs would be the output frequency/amplitude pairs for N sensors, where we expect the information to be contained in the pre-calibrated frequency versus sensor reading variation. The actual sensor values would be retrieved during ground processing making use of the pre-flight sensor calibrations with frequency. In one alternative scheme, one could derive the sensor values on the orbiter or the deltas from previous values, but such a scheme requires examination of the pros and cons. We then encode the data onto the telemetry for transmission back to Earth, with sufficiently low bit rates.

B. Transmission of Full 1 MHz Band (Lander to Orbiter to Earth)

One could alternatively (or concurrently) transmit the full 1-MHz band back to Earth. This would involve downconverting the full 1-MHz band centered about the down-converted carrier frequency, and digitally sample at the Nyquist rate. One would then encode with a rate $\frac{1}{2}$ error-correcting code, and then transmit the full data series back to Earth at 4 Msps as an example. On Earth, the data can be processed using various digital techniques to “dig out” the N frequencies for each of the sensor readings. Then, making use of the calibrated sensor reading versus frequency signatures, one recovers the sensor readings. Given that this is a very high data rate, the feasibility needs to be assessed on the Venus–Earth relay link in order to achieve this. One also needs to evaluate and accommodate on-board storage of the recorded data between orbits. Similar data rates used for interplanetary distances involved Mars Reconnaissance Orbiter (MRO) which made use only of Reed-Solomon encoding to achieve a 4.4 Mbps data rate using a hardware-limited 6 Msps. This data rate was used only during portions of cruise (prior to Mars arrival) and when Mars was at minimum distance to Earth [15]. One could also make use of a lower rate code (but with higher threshold) such as LDPC 7/8.

C. Lander to DSN DTE Link

Another option is to make use of a DTE link involving the AM radio transmitter on the surface of Venus to a DSN station on the surface of Earth. We again assume that the transmitted analog AM signal occupies a 1-MHz bandwidth with the carrier centered on 1 GHz¹ but this time only consider the case of 6 side-tones (sensor channels) falling within the 1-MHz band.

We again assume a 2-dB gain for the transmit antenna on Venus’ surface, and initially a very conservative 5-dB atmospheric attenuation due to the Venus atmosphere which should accommodate a lander elevation angle of 20 deg and above. A range distance of 0.5 AU was used in these links (for reference, the minimum distance between Venus and Earth is ~ 0.3 AU and the maximum is ~ 1.7 AU).

¹ Later, we will consider the case of an L-band signal link as some DSN stations have existing equipment to support this link frequency.

Given the relative geometry of Venus to Earth, a lander could be judiciously placed on the surface so that the elevation angle to Earth stays reasonably high (due to the slow rotation of Venus) so that visibility to Earth remains stable, allowing for much smaller Venusian atmospheric attenuation. Thus, for the DTE links, the surface features on Venus as seen from Earth should stay pretty much the same over the course of several days. For instance, during minimum Earth–Venus distance, the same face of Venus always faces the Earth. We can thus significantly relax the 5 dB Venus atmospheric attenuation perhaps down to 1 dB or even less [12] where the elevation angle from the lander to Earth is mostly about the zenith direction, say above 70 deg elevation. This will allow for greater margin or less required RF transmit power than is the case at 20-deg elevation angle. In addition, a DTE link involving an optimum selected site on Venus will allow for effectively 24-hr reception (coverage) of the transmitted signal by alternating between DSN sites as Venus sets at one site and rises at another. This is as opposed to the several-minute visibility per orbit for the cases involving the lander to an orbiter (see Sections III.A and III.B).

The DSN receiver configuration will utilize both a closed-loop receiver for the ever-present carrier (for monitoring purposes) and an open-loop receiver to capture the 1-MHz band centered at the carrier to allow for post-processing detection of the sideband tones (sensor channels). Using an open-loop receiver for the sidetones makes more sense since it is impractical to have a large number of closed-loop receiver channels to attempt real-time detection of the sidetones. In this case, margin will take on a different “flavor,” and we could go lower than 6 dB. Signal processing considerations include:

- 1) The number of seconds one can integrate to detect the signal energy, especially for margins near threshold.
- 2) How much the sensor reading frequency changes over a given integration time. This would make use of the pre-calibrated “sensor frequency versus sensor quantity” trend inferred from the Venus atmosphere simulator. One could get an estimate of “smearing” over the integration time.
- 3) The selected frequency bandwidth within a channel to integrate over, again making use of knowledge of the pre-calibrated sensor curve and guard bands.

For the first cases of link budgets, we considered both a single 34-m antenna and a single 70-m antenna for the receive antennas, where the low noise amplifier (LNA) systems are operated in a cooled environment. Arraying DSN antennas is another option for future considerations.

Given the much lower 1-GHz sky frequency (versus X-band or S-band), the beam of the receiving antenna is much wider and thus the contribution of Venus hotbody noise is significantly smaller at the stated range distance, and would be very small compared to receiver noise temperature and Earth atmospheric noise temperature increase contributions to the operating system noise temperature. This is as opposed to the surface-to-orbiter link where we conservatively assumed that the orbiter antenna beam footprint captures much of the ~600-K hotbody noise of Venus. We assume a closed-loop tracking loop bandwidth of 3 Hz for the carrier. This could be narrowed or widened depending upon the frequency stability of the lander’s reference oscillator and any fluctuations such

as due to atmospheric scintillation (which still needs to be quantified). We will evaluate the margins for the sideband channels based on a loop bandwidth of 3 Hz, although we would process these channels using post-processing tools on the open-loop data.

The 1-GHz capability does not currently exist at any of the DSN stations. However, at the 70-m stations, an L-band system does exist. The LNA output can be diverted to the L-band downconverter (versus the L-S “upconverter”) (~600 MHz wide) [16]. That output goes via fiber to the Radio Astronomy and Radar Group (RARG) and Signal Processing Center at Goldstone (SPC10). Thus, one could make use of a link frequency of 1.67 GHz. The L-band parameters are available from the DSN Telecommunications 810-005 document, and are utilized in the L-band link analysis discussed here. Such parameters include L-band gain and noise temperature coefficients [17] and L-band Earth atmosphere degradation parameters [18]. The resulting links at 1.67-GHz L-band involving a 70-m antenna are more optimistic than those making use of conservative assumptions in the 1-GHz links discussed previously.

Table 1 displays the transmit power levels required for a 3-dB margin on each sideband channel for the scenarios provided. Given the strict relationship between carrier power and sideband power for the given number of sidebands in AM radio, the carrier margin in all cases is about 14 dB, more than sufficient for maintaining carrier lock in a closed-loop receiver. This carrier margin does exceed the 6-dB (or 10-dB) margin policy values normally used for non-standard links where there is high uncertainty. The open-loop data will be post-processed to “dig” out the sidetone signals assuming an appropriate integration time and calibrated “sidetone frequency versus sensor reading” characteristic. Such techniques make use of spectrum analysis (integrating periodograms) or software PLL (where one can exercise different parameters such as loop-bandwidth and loop-update time) to detect signals. Much of this can be done on-board as part of the first scenario earlier discussed, as there are available flight processors that possess significant processing power and utilize dedicated DSP cores. Reasonable power levels on the lander could be utilized using the existing L-band system at the 70-m (last two rows of Table 1).

Table 1. Required transmitter power for various scenarios Involving Lander to DSN links with six sidetones (14 dB carrier margin; 3 dB sidetone margin).

Link Frequency (GHz)	DSN Antenna	Atmospheric Attenuation (dB)	Reqd. Trans. Power (W)	Comments
1	34-m	1	110	
1	34-m	5	280	
1	70-m	1	26	
1	70-m	5	65	
1.668	70-m	1	10	Existing System
1.668	70-m	5	25	Existing System

The required power levels in Table 1 could perhaps go much lower (by a factor of two) if we assume the lander antenna is peaked towards the vertical (near zenith) for the DTE links, where we could assume 5 dB gain instead of 2 dB.

Given that the span of the L-band receiver system is from 1.628 GHz to 1.708 GHz, frequency selection should consider avoiding interference with any existing assets at L-band. If we are considering an L-band DTE link at 1.67 GHz, we could also consider a nearby (in frequency) S-band link which should be “just as good.”

Another source of uncertainty is the frequency stability of the reference oscillator used on the lander. This will influence the loop bandwidth (LBW) required at the DSN receiver to capture the signal, given that there is a tradeoff between having to widen the LBW to capture all the signal energy versus shortening it to minimize the noise accepted into the loop.

As more sensors are added, the required transmit power levels will need to increase to accommodate maintaining the same margin in each sidetone link.

IV. Link Budget Analysis

Figure 6 displays an example Link Budget (lander-to-orbiter) which shows the case for 10 W of RF power and 100 sensor readings each with their own frequency band. We assume each sideband tone has the same modulation index. The carrier and individual sideband modulation indices follow the formulation of Equations 1–3 in Section II. Thus, for the 100 sensors assumed here, the individual sideband tone modulation indices are set

Venus Lander to Orbiter		Range, m		Altitude, m		
		622132.4		240000	1	GHz Frequency
Link Parameter		Unit	Design		20	deg Elevation
TRANSMITTER PARAMETERS		Value				
Total Transmitter Power	dBm	40.00		10	W RF Power	
Circuit losses	dB	-2.00		100	Number of sidebands	
Antenna Gain	dB	2.00		0.095	Sideband Mod Index	
Antenna Pointing Loss	dB	0.00		0.95	Effective Mod Index	
				5000	Hz Sideband Width	
EIRP	dBm	40.00				
PATH PARAMETERS						
Space Loss	dB	-148.33				
Atmospheric Attenuation	dB	-5.00				
RECEIVER PARAMETERS				Diameter	Efficiency	
Antenna Gain	dB	10.91		0.5	0.45	
Receiver Circuit Loss	dB	-2.00				
Pointing Loss	dB	-0.01		1	Pointing Error (deg)	
Polarization Loss	dB	-0.50		0.09	Pntg Error Term	
TOTAL POWER SUMMARY						
Total Received Power	dBm	-104.92		276.64	K	Tsc(K)
Noise Spectral Density	dBm/Hz	-169.17		876.64	K	Top(K)
Pt/No	dB-Hz	64.25		600.00	K	Venus
CARRIER PERFORMANCE						
Carrier Pc/No	dB	62.63				
Bandwidth	dB-Hz	10.00		10	Hz	
SNR	dB	52.63				
Recommended Detection SNR	dB	10.00				
Margin	dB	42.63				
SIDE BAND PERFORMANCE						
Sideband Power	dB-Hz	39.18				
Bandwidth	dB-Hz	10.00				
SNR	dB	29.18				
Recommended Detection SNR	dB	10.00				
Margin	dB	19.18				

Figure 6. Example lander-to-orbiter link budget – 10 W RF power, with 100 sidebands.

to 0.095 such that the effective overall modulation index, m_{eff} , lies below unity (in this case $m_{\text{eff}} = 0.95$) to minimize over-modulation. Here the individual sideband width is 5 kHz (including guard band regions). The link margins are shown for the carrier (42.6 dB), and for an individual sensor channel (19.2 dB) where we assume all sensor channels are the same. Future work would involve running the AM signal through a PLL simulation tool to examine the effect of any over-modulation or under-modulation on the carrier given the various parameters, such as number of channels, modulation indices, acquisition bandwidth, and loop update time. In the link budget of Figure 6, we have assumed a 2-dB noise figure on the receiver with a 290 K physical temperature, and the maximum possible 600-K hotbody noise added to this to obtain an overall system noise temperature of 877 K.

Table 2 provides a summary of the different power levels considered in the trade study for the lander-to-orbiter scenario along with the dimensions of the preferred transmit antenna (single patch), preferred receive antenna (2×2 patch array) and carrier and data channel margins for each case.

Table 2. Link margin summary with power, antenna dimensions, and margins (lander-to-orbiter).

Lander transmitter output power (W)	Transmitter maximum antenna dimensions and shape (cm)	Orbiter receiver maximum antenna diameter dimensions and shape (cm)	Orbiter receiver performance margins (dB)
2.5	Single patch: 18 cm \times 18 cm with 7 cm depth	2×2 Patch array: 36 cm \times 31 cm with 7 cm depth	Carrier = 36.6 Sideband = 13.3 (100 tones)
5	Single patch: 18 cm \times 18 cm with 7 cm depth	2×2 Patch array: 36 cm \times 31 cm with 7 cm depth	Carrier = 39.6 Sideband = 16.2 (100 tones)
10	Single patch: 18 cm \times 18 cm with 7 cm depth	2×2 Patch array: 36 cm \times 31 cm with 7 cm depth	Carrier = 42.6 Sideband = 19.2 (100 tones)

Figure 7 provides an example of a 1.668-GHz DTE lander to DSN link budget for the case of 6 sideband channels. The ~14-dB carrier loop margin exceeds the 6-dB or 10-dB conservative values dictated by margin policy when there is high uncertainty associated with the link, applicable for the closed-loop receiver. The lower 2.9-dB margin associated with the sidetone channel is provided as an example, but it is emphasized that the sidebands can be post-processed from concurrent open-loop data, where the signals can be “dug” out of the noise floor using various signal processing techniques, involving spectral analysis or software PLL with selection of parameters such as integration times and bandwidths. The 1 dB of atmospheric attenuation listed in Figure 7 is understood to be a combination of a Venus contribution (at a high Venus surface elevation angle) and an Earth contribution (at an Earth station elevation angle of 20°).

DOWNLINK: Lander to Earth					
		0.5 AU Range		1.668 GHz Frequency	
				20 deg Elevation	
Link Parameter	Unit	Design		90 Percent Weather	
TRANSMITTER PARAMETERS				Value	
Total Transmitter Power	dBm	40.00		10 W RF Power	
Circuit losses	dB	-0.10		6 Number of sidebands	
S/C Antenna Gain	dB	2.13		0.39 Sideband Mod Index	
Antenna Pointing Loss	dB	0.00		0.95 Effective Mod Index	
				83333 Hz Sideband Width	
EIRP	dBm	42.03			
PATH PARAMETERS					
Space Loss	dB	-254.37			
Atmospheric Attenuation	dB	-1.00			
RECEIVER PARAMETERS					
Earth Station Antenna Gain	dB	60.99			
Receiver Circuit Loss	dB	-0.10			
Pointing Loss	dB	0.00			
Polarization Loss	dB	-0.10			
TOTAL POWER SUMMARY					
Total Received Power	dBm	-152.56			
Noise Spectral Density	dBm/Hz	-183.09			
Pt/No	dB-Hz	30.53			
CARRIER PERFORMANCE					
Received Pc/No	dB-Hz	28.91			
Telemetry Suppression	dB	0.00			
Range Suppression	dB	0.00			
Carrier Loop Noise Bandwidth	dB-Hz	4.77			
Carrier Loop SNR	dB	24.14			
Recommended Detection SNR	dB	10.00			
Carrier Loop Margin	dB	14.14			
SIDEBAND PERFORMANCE					
Sideband Power	dB-Hz	17.67			
Bandwidth	dB-Hz	4.77			
SNR	dB	12.90			
Recommended Detection SNR	dB	10.00			
Margin	dB	2.90			

Figure 7. Lander to 70-m DSN link at 1.668 GHz.

V. AM Radio – Transmitted Power versus Number of Sensors Trade (lander-to-orbiter)

Figure 8 displays the resulting sideband link budget margin versus number of sensors for four different power levels: 1 W solid purple, 2.5 W solid gray, 5 W solid orange, and 10 W solid blue for the lander-to-orbiter link. Also shown are the margins for the carrier channel: 1 W dashed purple, 2.5 W dashed gray, 5 W dashed orange, and 10 W dashed blue. The solid black curve shows the required 10-dB margin level. It should be kept in mind that this trade may involve further refinements in the future. For instance, if we assume an omni-directional antenna (actually hemispherical) on the orbiter, then the margins may be reduced by about 10 dB. Reduction in the conservative atmospheric attenuation assumption may increase the margins a few dB.

All cases here show sufficient margin above 10 dB level except for the 1 W case at the highest number of sideband tones. Thus, from this trade, one could conclude that a 2.5 W transmit power would suffice for all of the sideband number cases considered here. Given a

95% effective modulation index, the 36.6 dB carrier margin is more than sufficient for on-board detection and tracking. Once the carrier is detected, on-board processing would have knowledge of where to search for signal energy (relative to the carrier) within each sensor's expected bandwidth limits. The resulting sensor signal strength and frequency would then be packaged for relay back to Earth on the DTE telemetry. One could perhaps make use of more than 100 sensors, but one should remain cognizant of the resulting margins as well as uncertainties of the various link budget entries such as for atmospheric attenuation, scintillation and hotbody noise. Such a trade involving required transmit power versus number of sensors should be carried out for the DTE link which so far only was considered for the case of six sensors.

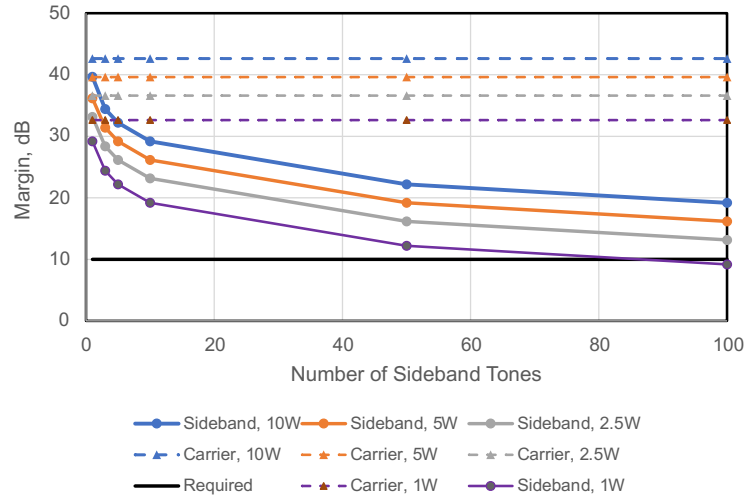


Figure 8. Lander-to-orbiter link margins for various power levels for sideband (solid curves) and carrier (dashed curves) as well as required 10 dB level (solid black curve).

VI. Concluding Remarks and Caveats

We have considered three options for conveying Venus surface sensor data back to Earth making use of analog radio technology for the surface lander radio system. These approaches involve: 1) a lander-to-orbiter link where the orbiter will perform specialized processing to extract sensor reading frequencies to be telemetered back to Earth via a DTE link; 2) a lander-to-orbiter link where the full 1 MHz bandwidth (after down-conversion) will be sampled, digitized, and encoded back to Earth for specialized processing involving signal extraction; and 3) a DTE link from the lander to the DSN where the received signal will be recorded on an open-loop receiver and post-processing will be employed to extract the sensor readings. The design of the approaches presented here are very preliminary and additional work is required. Some important points that require further investigation are itemized here.

- Intermodulation interference/harmonic distortion – As more sensors are employed, the appearance of intermodulation products may start to appear and their relative amplitudes relative to actual sideband tones will need to be characterized. Thus, a detailed study of the use of N sideband tones, their individual bandwidths, and

judicious placement of sensor tones will need to be conducted. One would also need to discern between harmonics and “true” tones.

- Bandpass response – One would need to characterize reduction of amplitude of the sideband tones over the 1 MHz bandpass due to response of transmitter (modulator, amplifier, etc.). That is, the outskirts near -0.5 MHz and $+0.5$ MHz may have significant loss (relative to center). Again, this could be remedied by extending the front-end bandwidth (say 1.5 MHz) and just making use of the central 1 MHz.
- Link budget uncertainties – We should maintain large margins for now to account for unforeseen additional losses or effects, along with several conservative assumptions in selecting parameter values. Thus, further analysis is needed as the link margin is desired to be kept high. Thus, we have assumed link margins of 10 dB to account for uncertainties for the lander/orbiter links. Possible link refinements could include considering the footprint of the receive antenna against the surface of Venus to refine the hotbody noise contribution (from its maximum value assumed) as well as relaxing the atmospheric attenuation placeholder.

We would need to understand how many different signals can be input to the modulator and what complexities would arise with a large number of sensor channels. This is a hardware consideration.

Instead of a double-sideband AM system (DSB) presented here, one could also consider the use of a single-sideband AM system (SSB), which has a bandwidth advantage, but does not have a power advantage over DSB [19]. A DSB system is thus superior to a SSB system given that the sidebands are coherent while the noise is not.

The use of an FM system was not considered in this study as the carrier frequency would vary in accordance with the modulating signals and we preferred to have an ever-present carrier frequency be at a known frequency for any given instant of time. However, one could make use of a pilot carrier if FM is considered in a later study.

The visibility during a particular orbit for the 240 km altitude would only be a few minutes, so the strategy of sending up the signal from the lander would need to be carefully designed, also taking the expected lifetime of the lander system into account. However, a DTE link could be maintained over several hours or several days by alternating tracks between DSN stations.

Given the high symbol rate (~ 4 Msps) of the open-loop DTE option, considerations must be accounted for in the Venus-to-Earth link from the orbiter (whether X-band or Ka-band), as well as with the on-board storage of the data between relay tracks and between orbits.

Acknowledgments

We would like to thank Larry Snedeker at Goldstone for information regarding the L-band equipment at the 70-m station. We would also like to thank the HOTTech program (sponsored by NASA Headquarters) for supporting this study and Jon Hamkins for

supporting editorial preparation work of this paper. We are indebted to Jim Lux for his very informative and meticulous comments, including those dealing with historical aspects of past systems prior to the advent of modern digital technology.

References

- [1] A. Court, “How hot is Death Valley?” *Geographical Review*, vol. 39, no. 2, pp. 214–220, April 1949. <https://doi.org/10.2307/211044>, <https://www.jstor.org/stable/211044>
- [2] Science Mission Directorate, “Technology Highlights 2016,” National Aeronautics and Space Administration, 2016. https://smd-cms.nasa.gov/wp-content/uploads/2023/04/NASA_2016SMD_Report_final_highres.pdf
- [3] <https://www.russianspaceweb.com/venera75.html>
- [4] T. Kremic, D. Vento, N. Lalli, and T. Palinski, “Extreme Environment Simulation - Current and New Capabilities to Simulate Venus and other Planetary Bodies,” 2014. <https://ntrs.nasa.gov/api/citations/20140013390/downloads/20140013390.pdf>
- [5] <http://www.svengrahn.pp.se/radioind/MVradio/MVradio.htm>
- [6] Range Commanders Council Telemetry Group, “Telemetry Standards”, IRIG Standard Document 106-20, Published by Secretariat, Range Commanders Council, US Army White Sands Missile Range, New Mexico 88002-5110, July 2020. 106-20_Telemetry_Standards.pdf (irig106.org)
- [7] K. M. Uglow, “Noise and Bandwidth in FM/FM Radio Telemetry,” *IRE Transactions on Telemetry and Remote Control*, pp 19–22, May 1957. <https://ieeexplore.ieee.org/document/6540509>
- [8] K. M. Uglow, “Analysis of DSB/FM Telemetry System Errors,” Report SC-CR-70-6092, Sandia Laboratories, Contract No. 72-8647, December 1970. [4082683](https://ntrs.nasa.gov/api/citations/197000040001/downloads/197000040001.pdf) ([osti.gov](https://ntrs.nasa.gov/api/citations/197000040001/downloads/197000040001.pdf))
- [9] W. K. Victor, H. L. Richter, and J. P. Eyraud, “Explorer Satellite Electronics,” National Aeronautics and Space Administration Contract No. NASw-6, Technical Release No. 34-12, January 29, 1960. <https://ntrs.nasa.gov/api/citations/19630040001/downloads/19630040001.pdf>
- [10] W. K. Victor and R. Stevens, “The Role of the Jet Propulsion Laboratory in Project Echo,” in *IRE Transactions on Space Electronics and Telemetry*, vol. SET-7, no. 1, pp. 20–28, March 1961. doi: 10.1109/IRET-SET.1961.5008747. <https://ieeexplore.ieee.org/stamp/stamp.jsp?tp=&arnumber=5008747>
- [11] https://www.arthurcollins.org/echo_1.php
- [12] C. F. du Toit, D. Everett, and R. D. Lorenz, “Modeling of Venus Atmospheric RF Attenuation for Communication Link Purposes,” 978-1-5386-6854-2/19/\$31.00 ©2019 IEEE.
- [13] NASA HOTTech Program (<https://www1.grc.nasa.gov/space/pesto/space-vehicle-technologies-current/high-operating-temperature-technology-hottech/>).

- [14] J. L. Jordan, G. E. Ponchak, P. Neudeck, and D. Spry, "First Iteration Communications Circuit for a Long-Lived In-situ Solar System Explorer (LLISSE)," *2020 IEEE Aerospace Conference*, Big Sky, MT, USA, 2020, pp. 1–11.
[doi: 10.1109/AERO47225.2020.9172708](https://doi.org/10.1109/AERO47225.2020.9172708)
- [15] D. K. Lee, "Mars Reconnaissance Orbiter Telecom Design Control Document," Revision A, JPL D-22724, MRO-26-591A, National Aeronautics and Space Administration, Jet Propulsion Laboratory, California Institute of Technology, Pasadena, California, July 18, 2005.
- [16] D. J. Hoppe, B. Khayatian, B. Lopez, T. Torrez, E. Long, J. Sosnowski, M. Franco, and L. Teitelbaum. "Broadband Upgrade for the 1.668-GHz (L-Band) Radio Astronomy Feed System on the DSN 70-m Antennas," *The Interplanetary Network Progress Report*, vol. 42-202, Jet Propulsion Laboratory, Pasadena, California, August 15, 2015.
https://ipnpr.jpl.nasa.gov/progress_report/42-202/202C.pdf
- [17] S. D. Slobin, "70-m Submit Telecommunications Interfaces," in *DSMS Telecommunications Link Design Handbook*, Doc. 810-005, Module 101, Rev. G, Jet Propulsion Laboratory, California Institute of Technology, Pasadena, California, 2019. <https://deepspace.jpl.nasa.gov/dsndocs/810-005/101/101G.pdf>
- [18] S. D. Slobin, "Atmospheric and Environmental Effects," in *DSMS Telecommunications Link Design Handbook*, Doc. 810-005, Module 105, Rev. E, Jet Propulsion Laboratory, California Institute of Technology, Pasadena, California, 2015.
<https://deepspace.jpl.nasa.gov/dsndocs/810-005/105/105E.pdf>
- [19] J. P. Costas, "Synchronous Communications," in *Proceedings of the IRE*, vol. 44, no. 12, pp. 1713–1718, December 1956. [doi: 10.1109/JRPROC.1956.275063](https://doi.org/10.1109/JRPROC.1956.275063)